Mercury and Beyond: Diode-Pumped Solid-State Lasers for Inertial Fusion Energy

C. Bibeau, R. J. Beach, A. Bayramian, J. C. Chanteloup,
C. A. Ebbers, M. A. Emanuel, C. D. Orth, J. E.
Rothenberg, K. I. Schaffers, J. A. Skidmore, S. B. Sutton,
L. E. Zapata, S. A. Payne, and H. T. Powell

U.S. Department of Energy

Lawrence
Livermore
National
Laboratory

October 19, 1999

DISCLAIMER

Mercury and Beyond:
Diode-Pumped Solid-State Lasers
for Inertial Fusion Energy

C. Bibeau, R. J. Beach, A. Bayramian, J. C. Chanteloup, C. A. Ebbers, M. A. Emanuel,
C. D. Orth, J. E. Rothenberg, K. I. Schaffers, J. A. Skidmore, S. B. Sutton,
L. E. Zapata, S. A. Payne, H. T. Powell

Lawrence Livermore National Laboratory
7000 east Ave. Livermore, CA 94550-9234 USA

Abstract

We have begun building the "Mercury" laser system as the first in a series of new generation diode-pumped solid-state lasers for inertial fusion research. Mercury will integrate three key technologies: diodes, crystals, and gas cooling, within a unique laser architecture that is scalable to kilojoule energy levels for fusion energy applications. The primary performance goals include 10% electrical efficiencies at 10 Hz and 100J with a 2-10 ns pulse length at 1.047 μm wavelength. When completed, Mercury will allow rep-rated target experiments with multiple target chambers for high energy density physics research.

1. Introduction

Gas-cooled, diode-pumped, Yb:crystal lasers are envisioned to be the next-generation ICF solid state laser system producing high energy per pulse at modest rep-rates. As a solid state laser system, this new design shares a number of common features with flashlamp-pumped glass laser systems, especially with regard to fundamental issues: multi-pass amplification, laser propagation, energy storage, extraction, pumping, linear and nonlinear wavefront distortions, frequency-conversion, and beam-smoothing. The diode-pumped solid state laser (DPSSL) approach builds on the last two decades of solid state laser development but also adds several imposing challenges -- repetition rate, reliability, and cost. Large scale flashlamp-pumped solid state lasers built for ICF studies have been optimized for the $/Joule figure-of-merit and for their ability to match the target requirements. They are inherently single-shot devices, requiring several hours to recover from thermal distortions. However, this limitation need no longer be imposed by the laser technologies conceptually assembled in the early 1980s by Krupke and Emmett.[1,2] Innovative solutions for building ICF lasers with high repetition rate and efficiency include:

- Trading the flashlamps for large, low-cost laser diode arrays
- Using Yb:crystals for greater energy storage and thermal conductivity than Nd:glass
- Employing near-sonic helium for cooling of the laser slabs

The laser diode arrays represent an enabling technology for realizing solid-state lasers for ICF. The reliability, brightness, and efficiency of laser diodes offer significant advantages over flashlamps. For ICF applications however, the performance specifications are more demanding than what is currently available and will require continued development over the next ten years. In addition, the diode array manufacturing costs will eventually have to be reduced by an order of magnitude through automation and mass production.

Yb:S-FAP crystals are being developed as an alternative crystalline gain media which offer high energy storage with a practical cross section. This material exhibits a 3x longer fluorescent lifetime and 2x larger emission cross section than Nd:glass. Research efforts at LLNL and elsewhere are currently underway to grow Yb:S-FAP crystals in large diameter boules (>7 cm). Eventually these efforts will need to be scaled to even larger diameters (20 cm) with high optical quality for beam apertures supporting kilojoule energies.

Gas cooled architectures, in which the laser slabs are mounted in vane elements supporting the gas-flow in which heat is extracted from the face of the laser crystal were previously demonstrated in small-scale experiments[3]. Gas-cooled laser architectures offer the promise of good beam quality due to minimal thermal distortion simultaneous with other essential parameters such as high peak power, rep-rated operation, high wall-plug efficiencies, and beam smoothness. Most importantly, this cooling technique is scaleable to larger aperture-size and hence greater energy per pulse.

The Mercury Laser is the first step in integrating these new approaches, and in producing new capabilities for irradiating ICF targets. These new facilities with rep-rated capability will provide a paradigm-shift from Nd:glass based laser system for experiments in high energy density physics. The primary performance goals for the Mercury Laser are:

- 10 Hz repetition rate
- 10 % efficiency
- 1.047μm wavelength (1ω)
- 2-10 nsec pulsewidths
- 100 Joules energy (1ω)
- 5x diffraction-limited beam quality
- 10^7 shot lifetime

When completed, Mercury (Fig. 1) will be the highest energy/pulse diode-pumped laser ever built by an order of magnitude. It is noteworthy that the 100 J energy is the same as that of the Janus Laser, which is based on flashlamp-pumped Nd:glass and originally built in 1973. In addition, the Mercury Laser will be upgradable to 3ω generation, broad bandwidth for beam smoothing, and picosecond pulse operation.
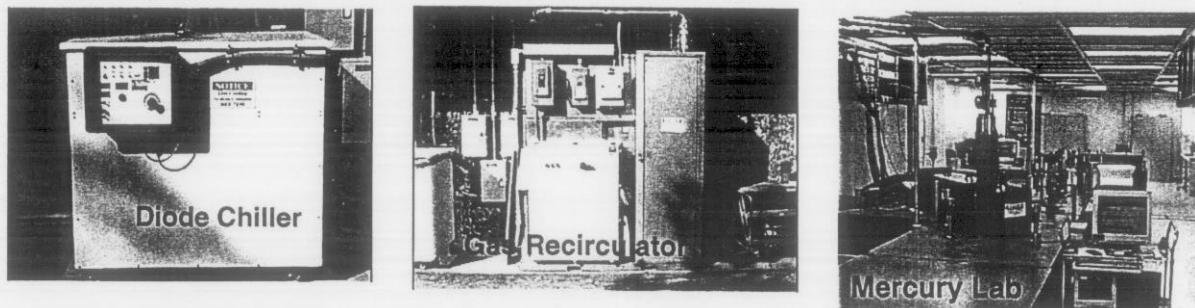

Fig. 1. Mercury laboratory and utilites.

2. Laser architecture and modeling

The Mercury laser design is predicated upon employing three technological advances: efficient and reliable diodes operating at 900 nm, Yb-doped crystals that offer longer storage lifetimes than the traditional Nd-doped materials, and active cooling with near-sonic helium gas flow across the crystalline laser slabs for rep-rated operation. The system layout incorporates an oscillator, pre-amplifier, and two power amplifiers. The gas-cooled power amplifiers are four-passed in an angular multiplexing scheme. An adaptive optic in the beamline will be used to correct for wavefront distortions incurred during amplification.
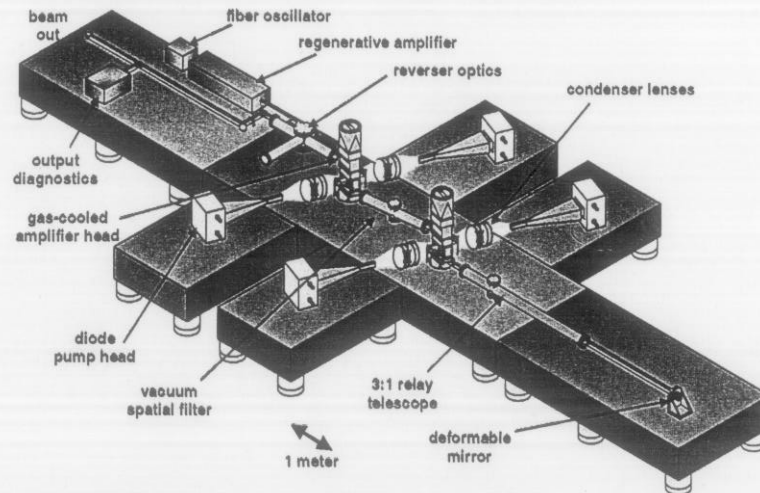

Fig. 2 Mercury laser schematic.

The amplifier head will be optically pumped from both sides. The dual pumping design allows for more uniform pumping and thermal loading on the crystals. The light from the diode array light is first concentrated with a hollow lens duct[4] followed by a hollow element that homogenizes spatial profile of the pump beam. Both the duct and the homogenizer are coated on the inside with a protected silver coating. The silver coating was chosen for its high reflectivity (>99%) at grazing incidence angles. The light emerging from the output of the homogenizer is imaged onto the gain media with a set of four condenser lenses designed to minimize the spatial aberrations. The angled dichroic beam splitters allow the pump beam to pass through the optic and into the amplifier head while allowing the extraction beam to be reflected. We have assembled one out of four pump delivery arms as shown in Fig. 2 below.

Fig. 2. Picture of one of four diode pump delivery arms.
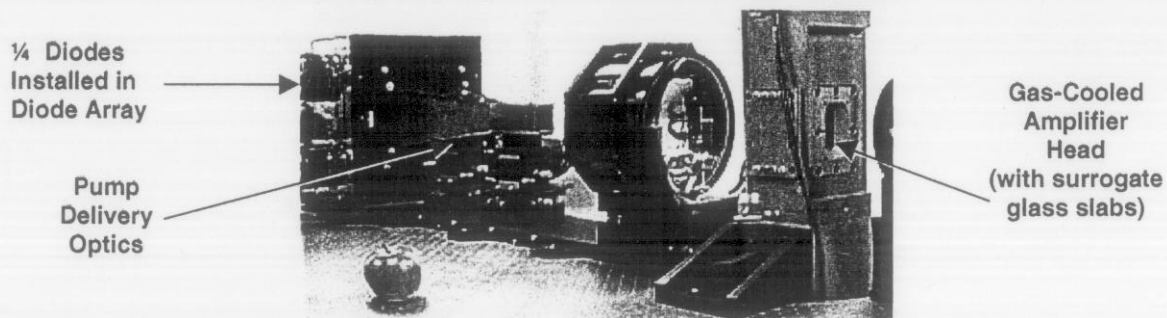
In order to fully test the amplifier head and pump delivery system this year, surrogate gain media (Nd:glass) was placed in the vane elements within the amplifier head. This allows us to test the pump delivery efficiency, pump light uniformity within the laser slabs, gas flow dynamics, and thermal deposition profiles. Once the Yb:S-FAP crystals are ready, we can easily

switch the surrogate slabs with the crystals. This approach will allow us to test the key elements in parallel with our efforts to develop adequately large crystals.

In addition to the experimental work we have also developed a series of codes to model the laser system performance. In particular we have developed a 1ω extraction code that includes:

- Effects of diode transient heating during the pump pulse, such as
  - roll-off in diode array output power,
  - red shift or diode chirp in the diode emission spectrum,
- A Gaussian distribution of wavelengths representing the spread in the center wavelengths of the approximately 6400 individual diode bars that will eventually comprise the entire pump array.
- A user definable pulse shape

The energetics code is used to normalize 2-dimensional pump deposition profiles at each slab, as well as slab edge-cladding optical loading values. This last portion of the code approximates the physics associated with the pump excitation process by using a 1-dimensional pump pulse propagation model. This propagation code dynamically calculates the gain loading of the individual laser slabs using a treatment that includes the effects of Yb^{3+} ground state depletion, spectrally selective pump wave depletion, Yb^{3+} fluorescence decay, and amplified spontaneous emission (which is handled using a simplified treatment). The code predicts that the pump volume and extraction beams are well overlapped at greater than 90% efficiency for all gain crystals.

Energy extraction modeling uses a standard Frantz-Nodvik analysis that has been modified to account for the quasi-three level nature of the Yb^{3+} ion to calculate the gain and extraction after each pass through the system. Included in the modeling is the impact of the narrow absorption feature on the pump excitation radiation. The integrated pump power spectrum after the slabs exhibits a spectral hole burned into it by the absorption of the Yb^{3+}:S-FAP. The final slab to be traversed by the extracting pulse is projected to see a fluence of 9 J/cm^2 (~3x saturation fluence). In addition the code also performs a path integral of the local extraction pulse irradiance, which is in turn used to calculate a B-integral for the system. One example of a sensitivity study is shown in Fig. 3, where both efficiency and output pulse energy are plotted against the pump pulse duration. In terms of pulse energy output and overall efficiency, the goal of the Mercury laser system is 100 J and a wall-plug efficiency of 10%. Using an assumed diode efficiency (electrical-to-optical) of 45% these goals can be met with a pump pulse duration of 750 μsec.
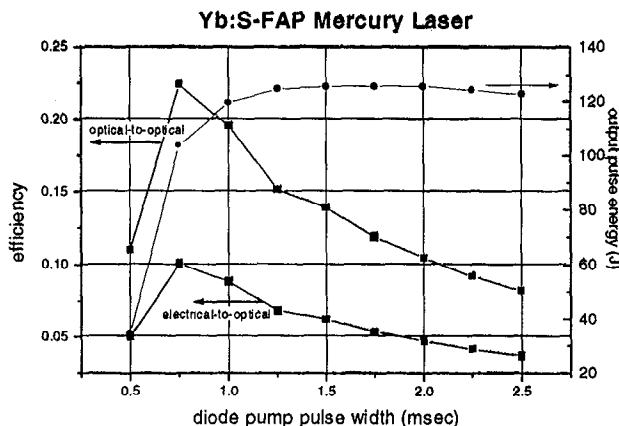

Fig. 3. Mercury laser system performance versus diode pump pulse duration.

3. Diodes

A critical technology for realizing inertial fusion energy is in the cost and efficiency of laser diode arrays. Existing diode technical performance specifications do not currently meet the demanding requirements of IFE. In addition, the manufacturing costs will have to be reduced by approximately two orders of magnitude to make IFE economically viable. Today, a significant fraction of the cost associated with fabricating laser diode arrays is attributed to "packaging." Our objective has been to develop a manufacturing approach that would reduce the mounting costs to ~50% of the cost of the diode. The laser diode array architecture allows 40 diode bars to be mounted in a single heatsink that is formed from a monolithic substrate that is thermally conductive but electrically insulating. The microlenses are pre-mounted in-house on a high-precision manufactured frame made of silicon.
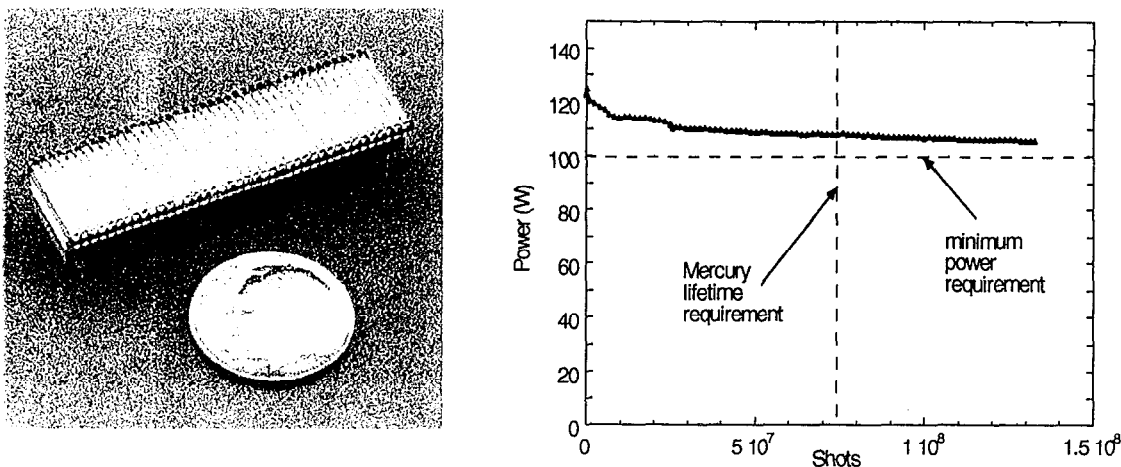

Fig. 4. (a) 900 nm 40-bar microlensed laser diode array. (b) Lifetest data for 900nm diode material. The material exhibits < 20% degradation over 10^8 shots under the Mercury conditions: 750 μs, 10 Hz operation.

Together with an industrial partner, Coherent-Tutcore, we made progress on the development of aluminum-free 900 nm laser diode bars. The growth conditions were changed in order to improve the spatial wavelength uniformity to ± 3 nm and to decrease the temperature sensitivity. Consequently, the power droop over a 750 μs pulse has also been reduced to less than 5% at the end of the pulse, which is well within previous expectations. We packaged, characterized and life-tested two 40-bar arrays of 900nm laser bars using this diode material as shown in Fig. 4. The array was operated up to 5 kW of peak power (1.25 kW/cm^2) with a slope efficiency of ~ 1.0 W/A (per bar), which gives a wall-plug efficiency of 45% at the design point (Fig. 5). We have received 2000 diode bars this year and mounted 400.

3.1 Diode backplane

We have designed and built a backplane that can mount up to 40 diode tiles with the following goals in mind: maintain maximum brightness, provide adequate thermal performance, allow for maintainability of the array, ensure mechanical/environmental protection of the diodes-all while maintaining a reasonable cost of fabrication. As shown in Fig. 6, each tile is designed to be modular for easy removal in the event of failure. To preserve brightness, the dead space between tiles is minimized to ~ 25% (to allow for lens frames, electrodes, and mechanical

tolerances). Electrical power is brought up through the backside of the backplane. The positive electrode attaches to one side of the tile, and all tiles share a common ground (i.e., the backplane itself). The deep, narrow channels in the backplane are necessary for reducing the thermal impedance of the system, $R_{th} \sim 1.2$ °C-cm^2/W. Despite the relatively low average power of the
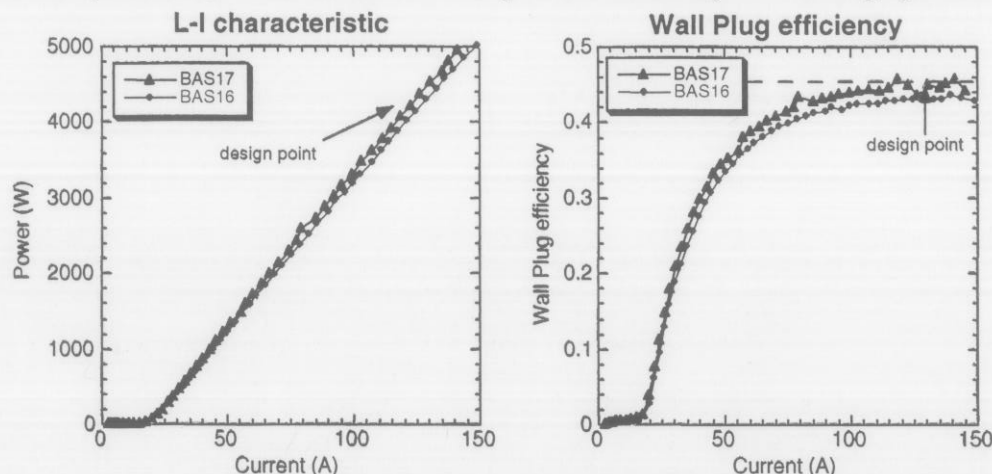

Fig 5. (a) L-I characteristic for 900 nm laser diode array. (b) Corresponding wall-plug efficiencies for these arrays.

diode bars under Mercury conditions, the thermal power dissipated is a serious issue for the performance/reliability of the diodes, as well as for preserving wavelength control. At the design point, the junction temperature of the diodes has a temperature rise of ~ 15 °C above room temperature for a single 750 μs pulse. High flow rates are used to prevent any significant caloric rise that would lead to thermal wavelength broadening across a row of adjacent tiles ($\Delta T < 1$°C, $\Delta\lambda < 0.3$ nm). The backplane is designed to operate from -40°C to 20°C in order to offset the steady state temperature rise. This wide temperature range allows for flexibility of repetition rate and wavelength tuning. To prevent condensation, the diodes are hermetically sealed and insulated by an outer enclosure that provides adequate thermal insulation, as well as mechanical protection of the diodes.
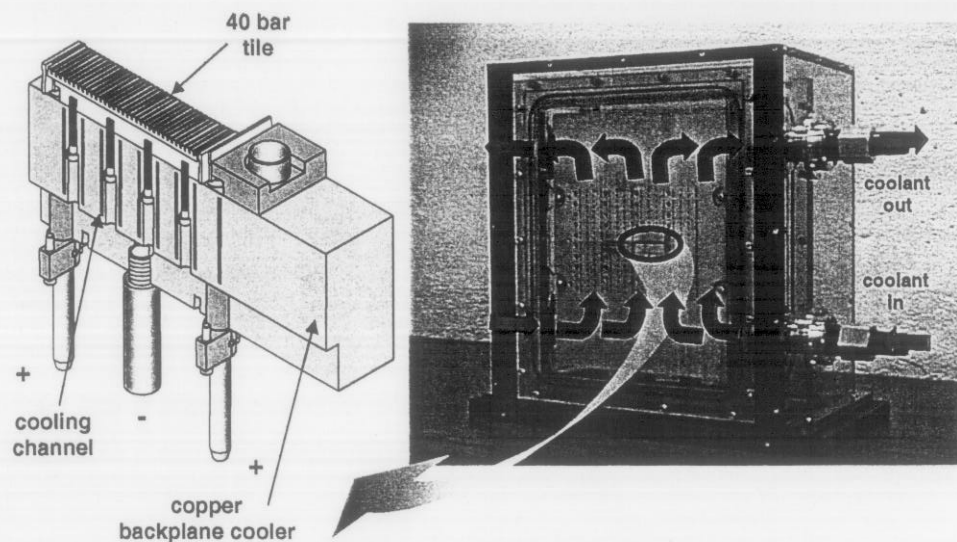

Fig. 6. Laser diode array backplane assembly

4. Amplifier head

The Mercury laser amplifier head and gas cooled architecture has been designed in a modular and scalable fashion, with the laser slabs mounted in an aerodynamic vane element as depicted in Fig. 7a. The vane elements are then stacked in a manner that forms a cooling channel between pairs of vanes, as depicted in Fig. 7b. Gas flows over the faces of the laser slabs, in the cooling channel, to remove the waste heat generated during the lasing process.[5,6] The assembled slab and vane cassette is then inserted into the amplifier head.
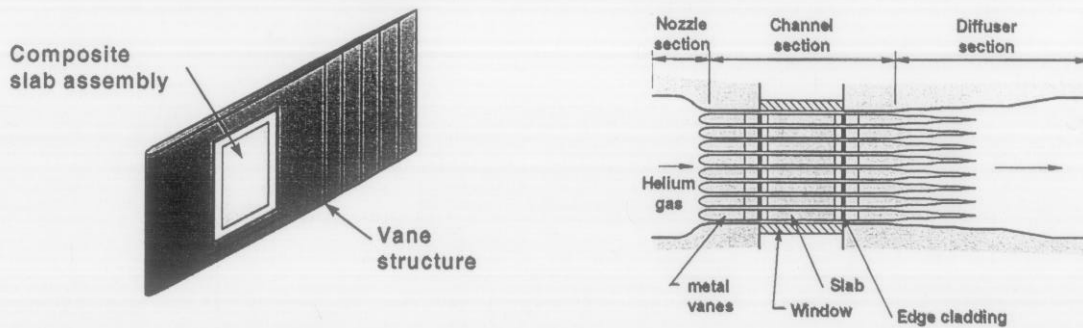

Figure 7. (a) Slab assembly embedded into the cooling vane structure. (b) A schematic cross-section through the amplifier head, showing the cooling passages between vanes.

The first laser head assembly was fabricated and installed in the Mercury laboratory, as shown in Fig. 2. Two types of vane elements were fabricated: Solid vanes are being used in initial flow tests to validate the aerodynamic design of the vane elements and the amplifier head. Vanes with cut-outs were fabricated to house the laser slabs, with a photograph of the fabricated hollow vane assembly shown in Fig 8a. The amplifier head and vanes were precision machined using the EDM process. Critical tolerances associated with the gas cooling channel profile, often as small as 0.0005 in, were achieved on both vane assemblies.

The bulk flow characteristics in the cooling channels located between vane elements were characterized at the design helium flow rate of 100 CFM using static pressure measurements at the channel inlet and exit. Measured pressure losses in the channel were nominally 0.8 ± 0.06 psi, as was expected from modeling. The channel-to-channel pressure loss imbalance was 0.019 psi (rms average). Preliminary analysis of this data indicates that the velocity imbalance in the vanes is no more than 3.5% of the nominal 100 m/s inlet velocity. This minor imbalance is not expected to cause flow instability problems in the amplifier head. Interferometry of glass surrogate glass slabs under gas flow was measured to be <0.2 waves/pass unpumped (Fig. 8b).
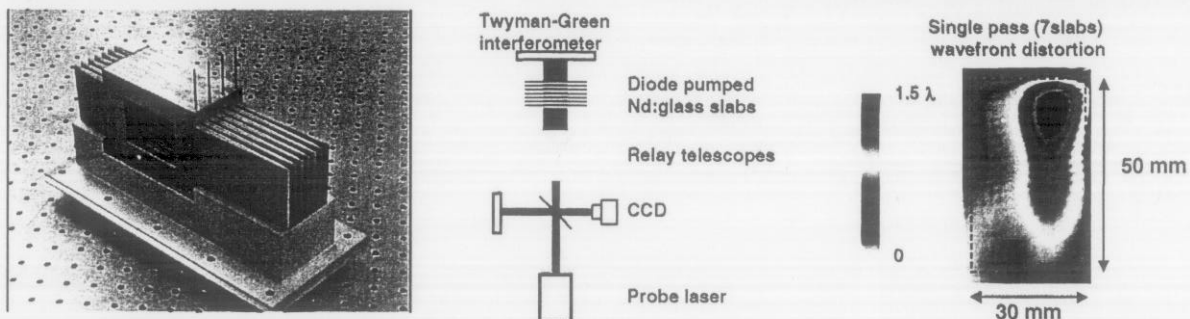

Fig. 8. (a) Picture of hollow vane cassette (b) Interferometry experiment and wavefront measurements with diode pumping over upper right quarter of the slab.

5. Crystal growth

Significant progress has been made in understanding the growth characteristics and defect chemistry of Yb:S-FAP [Yb^{3+}:$Sr_5(PO_4)_3F$] crystals. The Mercury laser requires crystalline slabs of dimension 4 x 6 x 0.75 cm. The growth of full size crystals has been a challenge due to a number of defects, including: cloudiness in as-grown boules, bubble core defects, grain boundaries, and cracking in larger diameter boules > 4.0 cm. An effort is underway to understand each of these defects and determine a reproducible growth technique for producing high optical quality crystals.

Over the last two years, methods to reduce or eliminate the defect structures in Yb:S-FAP crystals have been implemented or proposed. We have developed a way to remove the grain boundaries from the seed by "necking down" the crystal during the growth to propagate the defects out of the crystal; this technique has required the stabilization afforded by the closed-cycle chiller. At this time, significant progress has been made in understanding and controlling each of the defect structures in an effort to develop the growth of high optical quality Yb:S-FAP crystals. Results have produced boules with greatly reduced defects that have optical properties that nearly meet the Mercury specifications. The current plan is to produce high optical quality crystals of 4.5 cm diameter from which two half slabs can be cut and diffusion bonded together as shown in Fig. 9, to make adequately large crystals for Mercury.
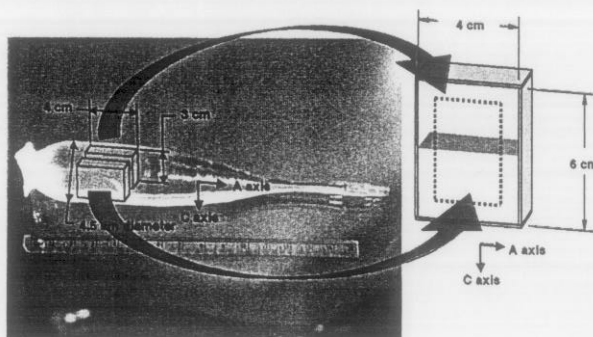

Fig. 9. Picture of Yb:S-FAP boule and orientation of the slabs for diffusion bonding.

5.1 Wavefront measurements of Yb:S-FAP crystals

We have measured a representative crystal of Yb:S-FAP on a phase-stepping interferometer using the P-HOM[7] technique. The P-HOM technique uses measurements of the reflected wavefront from both surfaces combined with the transmitted wavefront, to determine the bulk phase properties of a sample. Bulk phase measurements on a small apertured sample of the best quality 1 atomic percent (N = 2 x 10^{19} cm^{-3}) doped crystal grown to date, indicate the distortion to be only a few hundredths of a wave.

We also have shown that high quality crystals can be bonded together with nearly zero phase distortion due to the bond. We employ an angular bond technique to gradually overlap the two regimes so as not to create a step function effect. This bonding scheme accounts for possible errors in misorientation or differences in crystal homogeneity from slab to slab. Fig. 10a shows a phase map of an S-FAP crystal from which a refractive index core section has been removed from the middle and then the two outer pieces were diffusion bonded back together at an angle so as to create a smooth transition from one crystal to the other. Fig. 10b compares the 1-D

power spectral density plot (PSD) of one half of the crystal that does not include the bond to the 1-D PSD of the whole crystal including the bond. Clearly, the two 1-D PSD's show no measurable difference, thus validating this technique as an option for using sub-aperture crystals to produce a full-scale slab. We are also investigating a scheme where four sub-scale 2 x 3 cm sections of crystal are bonded together in a two-step process to produce the required crystal size.
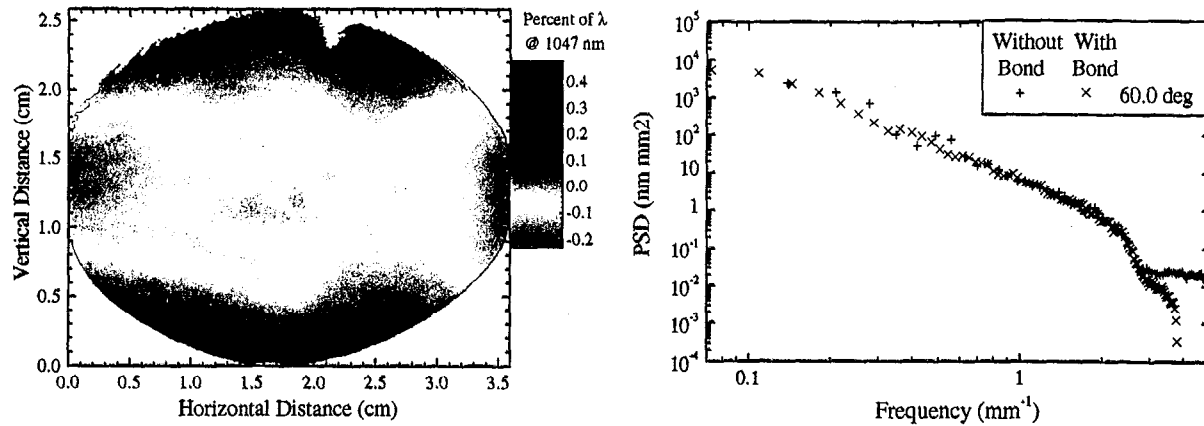

Fig. 10. (a) Phase map of a bonded Yb:S-FAP crystal. (b) PSD plot of bonded vs. unbonded Yb:S-FAP crystal showing PSD is unchanged.

6. Beam Smoothing

Calculations demonstrate that recently proposed crystalline laser gain media which are highly efficient, but narrow bandwidth (~0.3 THz in the UV), can provide adequate beam smoothing for direct drive ignition targets. By applying spectral shaping to the amplifier input and broad band frequency conversion with dual triplers, the gain narrowed bandwidth can be increased to ~1 THz. Such a laser amplifier (e.g. Mercury and its successors) is therefore promising for use as a driver in an IFE power plant.

A simple scaling of beam smoothing has been established which is helpful in the analysis of prospective ICF laser drivers. The essential result found is that the smoothing of low spatial frequency speckle relevant to direct drive is fundamentally determined by the product of the optical bandwidth and the illumination solid angle. Thus, a small bandwidth driver, by illuminating with a larger solid angle, can achieve smoothing equivalent to that of a larger bandwidth driver.

The scaling argument assumed can be used to compare NIF, for which it is generally agreed that 1 THz bandwidth will yield adequate smoothness for direct drive ignition, to the smoothing obtained with a proposed IFE driver with diode pumped crystalline (Yb:S-FAP) gain media of the same bandwidth. One finds that for a solid angle fraction of ~5% one can obtain smoothing significantly better than that of NIF. In this IFE driver configuration, the smoothness level obtained after an integration time on target of 1 ns is less than 0.07% for the modes of relevance to direct drive (ℓ-modes < 300).[8,9] Thus, one concludes that the bandwidth afforded by these crystalline gain media is adequate for direct drive IFE. In addition, higher bandwidth configurations such as beam lines operating at different optical frequencies (colors) can be considered to obtain further improved smoothing (rms 0.035% for ℓ<300).

7. Experiments on Mercury

Use of DPSSLs offers the option of high repetition rate (~10 Hz) or simply "shots-on-demand." This high rep-rated laser system could be fully exploited by employing multiple target chambers and multiplexing the laser beam between them. The high repetition rates will allow much more data averaging to reduce measurement errors, and will enable the exploration of chaotic behavior in plasmas, which is not addressable with a limited number of shots. It will also motivate the development of rep-rated targets and diagnostic capabilities. Extensive experimental studies can be executed to map out broad areas of parameter space. It also allows pump-probe experiments where the probe can be scanned in time to explore the detailed temporal response. This new approach could inspire a new generation of research on the basis of attaining new regimes of precision and understanding. Examples of experiments that could be enhanced with kilojoule-class DPSSL target-shooters offering "cheap shots" are:

- Precise equation of state (EOS) measurements
- Laser-plasma instability studies covering a broad range of parameter space including chaotic behavior
- Rep-rated 14 MeV neutron source development based on cluster fusion[10].
- Target diagnostics development for NIF utilizing x-rays and neutrons from solid targets
- X-ray laser backlighter development and optimization to probe high-density plasmas and targets
- Pre-staging subscale experiments prior to high-value execution on NIF
- Plasma studies such as Thompson scattering in high-pressure plasmas at high data collection rates
- Spatial tomographic three-dimensional X-ray imaging (0.1-10 MeV) for reconstruction of fine details

8. Beyond Mercury

A major objective of the present effort relates to establishing the readiness of the Mercury DPSSL driver to proceed to the next stage and beyond. The reliability, availability and maintainability of the laser components should be deemed to be acceptable for a future *integrated research experiment* or IRE (kJ-class laser coupled with average-power target chamber), and have a plausible means of attaining the driver requirements of inertial fusion energy (IFE)[11]. A possible program plan has been envisioned where efforts on NIF and fusion chamber research are included in the decision to proceed with the *engineering test facility* (ETF), an average-power fusion core. It is thought that addressing the IRE requirements will suggest a clear pathway for IFE DPSSL drivers for most issues, although the diode cost reduction will demand special attention. The specific long-term technology development areas can be summarized as follows:

- Increase the efficiency of the DPSSL IFE driver to between 10 to 20% by addressing improvements throughout the system.
- Reduce the cost of laser diode arrays to $0.50/watt for the IRE and define a pathway to $0.07/watt or less for IFE
- Devise and demonstrate a scheme to produce <1 % smooth irradiation on-target for direct-drive in 0.1-1 nsec.

- Grow gain media with > 10 cm aperture and fabricate into laser slabs with suitable optical quality (< 4 nm rms distortion for 0.002-2 cm spatial wavelengths).
- Demonstrate high-average-power frequency conversion with high efficiency (80 %) and suitable bandwidth, employing the gas cooling techniques.
- Produce beam quality of < 5x diffraction-limited using active and passive wavefront correction during average-power operation.
- Demonstrate integrated performance of DPSSLs to assure engineering viability with reliable operation, including the front-end, wavefront control, gas cooling, extraction, beam smoothing, and diode arrays.
- Develop approaches for a survivable target chamber where x-ray yields lead to significant surface ablation and where the final optic is suitably protected from debris and x-rays.
- Resolve the manner in which multiple apertures and beam bundles are assembled to attain the kilojoule and megajoule level.

One possible vision of an IRE is based on a 4 kJ DPSSL composed of four 1-kJ beamlets. This DPSSL would test performance at gain-limited aperture size as well as multi-aperture bundling technique needed to scale to very high energy. Most of the uses described above, including the neutron source, could be accomplished with the 4 kJ DPSSL of an IRE.

9. Summary

We have made progress this year towards component testing and activation of the Mercury Laser. We have built and tested one of four diode pump delivery arms. Ten, 40-diode bar tiles were installed and used to measure efficiencies of the optical diode pump delivery system. Wavefront of the amplifier head with surrogate glass slabs installed has been measured and gain measurements are currently underway. We also plan to validate pump and thermal wavefront computer models. During the next year we will focus on building one half of the laser system (one amplifier head pumped by two diode arrays) including the front-end injection laser. Small-scale extraction experiments are planned.

When completed Mercury will be the highest energy/pulse diode-pumped laser ever built by an order of magnitude that offers the dimension of high repetition rate (~10 Hz) or simply "shots-on-demand." The high repetition rates will allow much more data averaging and enable the detailed exploration of laser plasma interactions, which are not addressable with a limited number of shots. It will also motivate the development of rep-rated targets and diagnostic capabilities. Extensive experimental studies can be executed to map out broad areas of parameter space, in contrast to the relatively limited nature of data acquired in the past. In addition, a major objective of the Mercury laser relates to establishing the readiness of the Mercury DPSSL driver to proceed to the next stage and beyond for fusion energy.[1] A plan for a future *integrated research experiment* or IRE (kJ-class laser coupled with average-power target chamber) that meets driver requirements of a beamline for inertial fusion energy (IFE) has been prepared.

References:

[1]. W. F. Krupke, Fusion Technol. **15**, 377 (1989).

[2]. J. L. Emmett and W. F. Krupke., Sov. J. Quantum Electron. **13**,1 (1983).

[3] C. D. Marshall, L. K. Smith, S. Sutton , M. A. Emanuel, K. I. Schaffers, S. Mills, S. A. Payne, W. F. Krupke, B.H.T. Chai, OSA TOPS on Advanced Solid-State Lasers, **1**, 276 (1996).

[4]. R. J. Beach, Appl. Opt., **35**, 2005 (1996).

[5]. S. B. Sutton and G. F. Albrecht, J. Appl. Phys. **69**, 1183 (1991).

[6]. G. F. Albrecht, et al., Appl. Opt. **29**, 3079 (1990).

[7]. See for example, Measurement of the inhomogeneity of a window, Chaiyu, Ai and James E. Wyant, Optical Engineering, **30**(9), 1399 (1991).

[8] S. V. Weber, H. E. Dalhed, D. Eimerl, M. H. Key, S. M. Pollaine, J. E. Rothenberg, and C. P. Verdon, "Direct-Drive Capsules for NIF," ICF Quarterly Report **7**, 44 (1998).

[9] S. E. Bodner, D. G. Colombant, J. H. Gardner, R. H. Lehmberg, S. P. Obenschain, L. Phillips, A. J. Schmitt, J. D. Sethian, R. L. McCrory, W. Seka, C. P. Verdon, J. P. Knauer, B. B. Afeyan, and H. T. Powell, Phys. Plasmas **5**, 1901 (1998).

[10]T. Ditmire, J. Zweiback, V. P. Yanovsky, T. E. Cowan, G. Hays, and K. B. Warton, Nature, **398** 489, (1999)

[11]. C. D. Orth, S. A. Payne, and W. F. Krupke, Nuclear Fusion **36**(1), 75 (1996).